Measuring Economic Growth With A Fully Identified Three-Signal Model

Andrea Civelli* Arya Gaduh† Ahmed Sadek Yousuf ‡

University of Arkansas *University of Arkansas, NBER* *Aix-Marseille School of Economics*

Abstract

We augment Henderson et al. (2012)'s two-signal model of true GDP growth with a third signal to overcome its underidentification problem. The additional moment conditions from the third signal help fully identify all model parameters without ad-hoc calibrations of the GDP's signal-to-noise ratio. We characterize the necessary properties of the third signal. Using the model, we recover the optimal weight of official GDP in the composite true GDP growth estimates, which varies with the quality of the national statistics. The model improves on existing methodologies that use signals to measure true income.

Keywords: Remote sensing; Nighttime lights; Urban expansion; Economic activity measurement.

JEL Classification: E01, O11, O47, O57.

*University of Arkansas, Walton College of Business, Department of Economics, Business Building 402, Fayetteville, AR. Email: andrea.civelli@gmail.com.

†University of Arkansas, Walton College of Business, Department of Economics, Business Building 402, Fayetteville, AR. Email: agaduh@walton.uark.edu.

‡Email: ahmed-sadek.yousuf@univ-amu.fr.

1 Introduction

The seminal paper of Henderson et al. (2012) (HSW, henceforth) introduced a statistical framework to use nightlights growth to proxy for economic activity. HSW use this framework to obtain two main results. First, they show that nightlights can be used to directly predict GDP growth. This is useful, for instance, at sub- or supra-national level when official GDP measures are not available. A large body of literature has exploited this result for a variety of empirical applications.[1]

Second, they propose a model that combines official GDP — intended as a noisy signal of true economic growth — with nightlights as a second signal to improve estimates of unobservable true GDP growth. This is useful when official GDP measures exist, but there are reasons to believe they are unreliable (see e.g. Morris and Zhang, 2019). Their two-signal model of true GDP growth, however, has an important shortcoming: it needs to identify four structural parameters with only three sample moments from observed data. HSW solve this by assuming a value for the signal-to-noise ratio of the GDP signal.

The need for underlying conventional GDP data and the lack of a straightforward identification strategy have restricted the empirical applications of this model. Nevertheless, estimating true economic activity is, in principle, more relevant than just having an estimate of official GDP, and a fully identified model can constitute a useful benchmark for other approaches that aim to measure economic activity. This paper proposes a novel solution that overcomes the underidentification problem of the HSW framework by augmenting it with a third signal.

We first theoretically demonstrate that a three-signal version of the HSW model is fully identified. The third signal increases the number of parameters to be estimated; however, it also provides three additional moment conditions: its variance and covariances with the two original signals (official GDP and night-

[1] See, among the others, Storeygard (2016); Michalopoulos and Papaioannou (2013a,b); Alesina et al. (2016); Dreher and Lohmann (2015); Civelli et al. (2018); Hodler and Raschky (2014).

lights). The six moment conditions fully identify the six model parameters. We also characterize the necessary properties of this third signal.

Then, we illustrate its applications using urban land cover data as an example of a viable third signal. Globally, urban land cover data have become increasingly available for extended periods and at different frequencies. They have been shown to provide meaningful information about economic growth beyond nightlights, especially in more agriculture-intensive regions and at the subnational level (see, for instance, Goldblatt et al., 2019; Keola et al., 2015; Wu et al., 2013). Hence, it constitutes a convenient (albeit, not the sole) candidate for a third signal.

We show that urban land cover is a good candidate for a third signal in two samples of national economies: all and African countries. We first show that changes in urban land cover have a significant predictive power of official GDP growth. Then, we apply the urban land cover change to the augmented model and proceed to fully identify the model for the estimation of true GDP growth. We verify that it empirically satisfies the necessary properties to be a valid auxiliary signal.

We find that the relative weight of the official GDP data in the true GDP composite (λ^*, following the HSW notation) is 0.56 for the full set of countries. λ^* drops to 0.20 for the sub-group of countries with low-quality official GDP data and increases to 0.82 for countries with high-quality ones. For African countries, we find a $\lambda^* = 0.38$. Overall, they suggest that this method assigns an official GDP weight that is inversely related to the quality of the official data, as hypothesized by HSW.

Our approach is useful for empirical researchers in four ways.

First, as we show below, when feasible, this model is superior to simply using the additional signal as a covariate to improve *predicted GDP growth* (as in e.g., Baragwanath et al., 2021; Engstrom et al., 2021; Goldblatt et al., 2019; Lehnert et al., 2020). We find that the true GDP growth estimates from an identified two- or three-

signal model do not significantly differ. Similarly, once the key model parameter λ^* is recovered from a fully identified model, the true GDP growth estimates are invariant to using two or three signals in the GDP prediction stage.

Second, the fully identified model introduces new ways to improve true GDP estimates. The identified primitives for a set of regions where an appropriate third signal is available can be used to estimate true income growth in similar regions where such a signal is unavailable.[2]

Third, our approach can be used to validate the use of nightlights or other types of signals to predict economic activities, by providing a useful tool to assess the magnitude and direction of potential measurement errors. We find that these errors can be quite large, especially at the extremes of the income distribution and when true GDP growth is negative.

Finally, it provides a criterion to choose between alternative third signals, based on the minimization of the variance of true GDP growth forecast errors. This is empirically useful given the increasing availability of geospatial and other data that can serve as a potential signal. We illustrate its use by benchmarking urban land cover against nitrogen dioxide (NO_2) emission, another good predictor of true GDP growth (Morris and Zhang, 2019).

We contribute to the literature on methodological improvements to HSW's use of signals to measure true GDP growth. A strand of this literature highlights the non-linear aspects of the relation between nightlights and underlying economic activity (Bickenbach et al., 2016; Bluhm and McCord, 2022; Chen and Nordhaus, 2011; Goldblatt et al., 2019; Keola et al., 2015; Maldonado, 2022; Wu et al., 2013). Another focuses on the utility of different sources of nightlights and other satellite data – especially in conjunction with machine learning methodologies – to improve growth measurements (Baragwanath et al., 2021; Beyer et al., 2018; Dai et al., 2017;

[2]This result requires an assumption (used by HSW, in their calibration exercise, see p. 1009, 1018) that these two region groupings only differ from one other in their signal-to-noise ratio of the official GDP data.

Engstrom et al., 2021; Gibson and Boe-Gibson, 2021; Goldblatt et al., 2019; Lehnert et al., 2020; Wang et al., 2019; Zhang and Gibson, 2022).

Our work is closer in spirit to Morris and Zhang (2019) and Ezran et al. (2023) who rely on multi-signal settings to overcome the identification problem. Their models are based on econometric settings where the additional signals are used as instrumental variables, with significant deviations from HSW. We take a novel approach that introduces a simple theoretical refinement to significantly improve the HSW framework.

We also contribute a simple tool to aid empirical studies that uses nightlights to estimate socioeconomic developments. The list of topics that have been studied empirically based on nightlights data is long and growing.[3] Our approach provides a simple methodology to fully implement the HSW model in a way that minimizes the uncertainty around the optimal estimate of economic activity produced by the model. This is of paramount importance for all types of empirical applications.

The rest of the paper is organized as follows. Section 2 presents our theoretical refinement of HSW's two-signal model with the addition of a third signal. It is followed by the application of the method using urban land cover as a third signal. Section 3 describes the data followed in Section 4 by the empirical results for all and African countries. Section 5 illustrates the value of this fully identified model for empirical work. We conclude in Section 6.

[3]Nightlights have been employed, among others, to validate statistical measures of income, such as the Penn's World Tables or household surveys (Pinkovskiy and Sala-i Martin, 2016a,b); to estimate informal economic activities (Chen and Nordhaus, 2011; Ghosh et al., 2010); to study the effects of intercity linkages, institutions and ethnic characteristics on regional income in Africa (Alesina et al., 2016; Michalopoulos and Papaioannou, 2013a,b; Storeygard, 2016); to explore regional political favoritism (Hodler and Raschky, 2014); and to estimate the impact of aid on growth at sub-national level (Civelli et al., 2018; Dreher and Lohmann, 2015).

2 A Three-Signal Model of Economic Activities

2.1 The Underidentification of the Two-Signal Model

We begin by briefly recapitulating HSW's original model to estimate the true, but unobservable, GDP growth by exploiting two observable noisy signals correlated with the true economic activities. Let y_j be the true GDP growth rate in country j. Let x_{1j} and x_{2j} respectively indicate the two signals used in the model, which correspond to the growth rates of official GDP and of observed nightlights in country j in the empirical exercise. HSW assume that the two signals are linearly related to true GDP which, as standard in the signal extraction literature, allows for an error orthogonal to y_j that embeds the precision (or tightness) of the signal around the fundamental, namely:

$$x_{1j} = y_j + \varepsilon_{1j} \tag{1}$$

$$x_{2j} = \beta_{x_2} y_j + \varepsilon_{2j}. \tag{2}$$

The variance of y_j is denoted by σ_y^2. Similarly, the variances of the signals are given by $\sigma_{x_1}^2$ and $\sigma_{x_2}^2$. A similar notation is used for the variances of the signal noises as well: σ_1^2 and σ_2^2 for ε_{1j} and ε_{2j}.

HSW complete the model with a predictive equation that links the two signals to each other:

$$x_{1j} = \psi_{x_2} x_{2j} + e_j. \tag{3}$$

The predicted value $\hat{x}_{1j} = \hat{\psi}_{x_2} x_{2j}$ is linearly combined with the observed signal x_{1j} to improve the accuracy of the estimate of the true GDP growth exploiting the information contained in the signals:

$$\hat{y}_j = \lambda x_{1j} + (1 - \lambda)\hat{x}_{1j}. \tag{4}$$

The optimal weight on the official GDP in (4), denoted λ^*_{HSW}, is chosen to minimize the variance of the forecast error of the predicted GDP growth, $var(\hat{y}-y)$, given the structure of the model and the assumption that the errors in the measurement equations (1)-(2) are mutually orthogonal.

HSW show that λ^*_{HSW} is a function of four unknown parameters, namely $(\sigma^2_y, \sigma^2_1, \sigma^2_2, \beta_{x_2})$. From equation (8) of HSW, the solution is:

$$\lambda^*_{HSW} = \frac{1}{1 + \left(\frac{\sigma^2_1}{\sigma^2_y} + \frac{\sigma^2_1}{\sigma^2_2}\beta^2_{x_2}\right)}. \tag{5}$$

However, only three moment conditions are available from the observable data. Two conditions are obtained from the variance of the signals:

$$\sigma^2_{x_1} = \sigma^2_y + \sigma^2_1$$
$$\sigma^2_{x_2} = \beta^2_{x_2}\sigma^2_y + \sigma^2_2,$$

while the last one is provided by the covariance between the two signals, $\sigma_{x_1x_2}$:

$$\sigma_{x_1x_2} = \beta_{x_2}\sigma^2_y$$

To close the model and solve for the true income growth, they make use of the signal-to-noise ratio associated with signal x_{1j}, the officially measured GDP growth rate. From equation (1), define the signal-to-noise ratio as:

$$\phi = \frac{\sigma^2_y}{\sigma^2_y + \sigma^2_1}. \tag{6}$$

HSW split the sample of developing countries into two groups based on the quality of their national accounting system, and assume they only differ by the signal-to-noise ratio, ϕ. If ϕ for one group (say, those with high-quality data) is known, they

can use this equation to infer the ϕ for the other, and the optimal λ^*_{HSW}'s for both groups. HSW's preferred estimates of true income growth assume $\phi = 0.9$ for the high-quality data countries and conduct an insightful investigation of the relation between signal precision and λ^*_{HSW}; nevertheless, the underlying identification issue remains as any ϕ would in principle be admissible.

2.2 A Third Signal to Solve Them All

We demonstrate below that a third signal can overcome the underidentification of model parameters and do away with the need to assume a value for ϕ. Let the third signal be x_{3j}, corresponding to the growth rate of urban land cover in the empirical exercise in Section 4. We modify the structure of the model in two ways. First, we add to (1) and (2) a measurement equation for the new signal:

$$x_{3j} = \beta_{x_3} y_j + \varepsilon_{3j}. \tag{7}$$

We denote the variance of x_{3j} and ε_{3j} with $\sigma^2_{x_3}$ and σ^2_3 respectively.

Second, the predictive equation (3) is modified to also include the third signal:

$$x_{1j} = \psi_{x_2} x_{2j} + \psi_{x_3} x_{3j} + e_j, \tag{8}$$

which is associated to a predicted value of the main signal given by $\hat{x}_{1j} = \hat{\psi}_{x_2} x_{2j} + \hat{\psi}_{x_3} x_{3j}$.

As in the two-signal model, the optimal λ^* of the augmented model is chosen to minimize the variance of the forecast error of the predicted GDP growth. Using (8) in (4), the structural equations (1)-(2), and (7) and the assumption that

their errors are mutually orthogonal, $var(\hat{y}-y)$ can be written as

$$\begin{aligned} var(\hat{y}-y) &= var\big[\lambda(x_{1j}-y_j)+(1-\lambda)(\hat{x}_{1j}-y_j)\big] \\ &= \lambda^2\sigma_1^2+(1-\lambda)^2\big[\hat{\psi}_{x_2}^2\sigma_2^2+\hat{\psi}_{x_3}^2\sigma_3^2+(\hat{\psi}_{x_2}\beta_{x_2}+\hat{\psi}_{x_3}\beta_{x_3}-1)^2\sigma_y^2\big], \end{aligned} \tag{9}$$

Its derivative with respect to λ yields:

$$\lambda^* = \frac{\hat{\psi}_{x_2}^2\sigma_2^2+\hat{\psi}_{x_3}^2\sigma_3^2+\big(\hat{\psi}_{x_2}\beta_{x_2}+\hat{\psi}_{x_3}\beta_{x_3}-1\big)^2\sigma_y^2}{\sigma_1^2+\hat{\psi}_{x_2}^2\sigma_2^2+\hat{\psi}_{x_3}^2\sigma_3^2+(\hat{\psi}_{x_2}\beta_{x_2}+\hat{\psi}_{x_3}\beta_{x_3}-1)^2\sigma_y^2}. \tag{10}$$

It is easy to show that the OLS estimates $\hat{\psi}_{x_2}$ and $\hat{\psi}_{x_3}$ return a biased estimate of the inverse of the two coefficients β_{x_2} and β_{x_3}, with a bias structure that depends on the underlying parameters of the signaling model.[4] Using this fact and after a few manipulations, λ^* in (10) can be simply expressed as:

$$\lambda^* = \frac{1}{1+\Big(\dfrac{\sigma_1^2}{\sigma_y^2}+\dfrac{\sigma_1^2}{\sigma_2^2}\beta_{x_2}^2+\dfrac{\sigma_1^2}{\sigma_3^2}\beta_{x_3}^2\Big)}. \tag{11}$$

Therefore, the optimal λ^* depends on six unknown parameters $(\sigma_y^2, \sigma_1^2, \sigma_2^2, \sigma_3^2, \beta_{x_2}, \beta_{x_3})$. Six sample moment conditions are necessary to fully identify these six parameters from the data.

The first three condition are obtained from the variance of the three signals,

[4]The bias structure is given by:

$$\begin{aligned} plim(\hat{\psi}_{x_2}) &= \frac{1}{\beta_{x_2}}\left(\frac{\beta_{x_2}^2\sigma_y^2\sigma_3^2}{\beta_{x_2}^2\sigma_y^2\sigma_3^2+\beta_{x_3}^2\sigma_y^2\sigma_2^2+\sigma_2^2\sigma_3^2}\right) \\ plim(\hat{\psi}_{x_3}) &= \frac{1}{\beta_{x_3}}\left(\frac{\beta_{x_3}^2\sigma_y^2\sigma_2^2}{\beta_{x_2}^2\sigma_y^2\sigma_3^2+\beta_{x_3}^2\sigma_y^2\sigma_2^2+\sigma_2^2\sigma_3^2}\right). \end{aligned}$$

which using (1)-(2) and (7) can be expressed as:

$$\sigma_{x_1}^2 = \sigma_y^2 + \sigma_1^2 \tag{12}$$

$$\sigma_{x_2}^2 = \beta_{x_2}^2 \sigma_y^2 + \sigma_2^2 \tag{13}$$

$$\sigma_{x_3}^2 = \beta_{x_3}^2 \sigma_y^2 + \sigma_3^2. \tag{14}$$

The other three conditions are provided by the covariances between the three signals. These can be expressed as:

$$\sigma_{x_1 x_2} = \beta_{x_2} \sigma_y^2 \tag{15}$$

$$\sigma_{x_1 x_3} = \beta_{x_3} \sigma_y^2 \tag{16}$$

$$\sigma_{x_2 x_3} = \beta_{x_2} \beta_{x_3} \sigma_y^2 \tag{17}$$

Conditions (15)-(17) give the solution for β_{x_2}, β_{x_3}, and σ_y^2. Given these, (12)-(14) allow us to solve for σ_1^2, σ_2^2, and σ_3^2. We explicitly derive the model solution in Appendix B.1.

The third signal provides three new moment conditions — equations (14), (16), and (17) — with the introduction of two additional parameters (β_{x_3} and σ_3^2). It therefore overcomes the underidentification issue of the two-signal model. Two of these moment conditions are equivalent to those related to signal x_2 in HSW, and they are respectively obtained from the variance of signal x_3 in (14) and the covariance between x_3 and x_1 in (16). The additional moments from the covariance between x_3 and x_2 in (17) ensures that the model is (just-)identified.[5]

The solution to the three-signal model also allows us to recover the primitive parameters necessary to estimate λ_{HSW}^* for the two-signal model in (5). Hence, we can use equation (6) to infer true growth for the whole sample, even if the addi-

[5]In Appendix B.2, we show that the moment conditions from additional signals beyond the third lead to an over-identified model under the assumption of the orthogonality of the errors in the measurement equations. However, finding extra signals that satisfy the identification requirements (Section 2.3) is nontrivial.

tional signal is only informative for a subset of the sample for a given period. The ϕ for the sample where the third signal is informative would be sufficient to also pin down ϕ and λ^*_{HSW} for the rest of the sample. This largely simplifies the search for an empirically suitable third signal for the full sample in all periods.[6]

2.3 Identification Requirements for Signal Selection

For identification, signals must satisfy two conditions. First, the errors of the measurement equations (1), (2), and (7) (hereafter, the ME errors) are assumed to be orthogonal:

$$\sigma_{ij} = 0 \quad \forall i, j = 1, 2, 3; i \neq j. \tag{18}$$

This is a fairly common assumption in signaling models: HSW's two-signal model assumes $\sigma_{12} = 0$ (for official GDP and nightlights). Failing these conditions, additional covariance terms would show up in the expression for $var(\hat{y} - y)$, and the model would again be under-identified.

Second, for a solution to exist, the covariance between the second and third signals must be positive and sufficiently strong, i.e.:[7]

$$\sigma_{x_2 x_3} > 0 \tag{19}$$

$$\sigma^2_{x_1} > \frac{\sigma_{x_1 x_3}\sigma_{x_1 x_2}}{\sigma_{x_2 x_3}}. \tag{20}$$

The new signal must be sufficiently informative: it must be not only correlated with economic activity, but also with the main signals.

3 Data

We need data for the three signals: urban land cover, night lights, and official GDP.

[6] See Appendix B.3 for a full derivation of the solution for this split-sample approach.
[7] We detail these conditions in Appendix B.1.

3.1 Urban Land Cover

Our measure of urban land cover is obtained from the European Space Agency (ESA) Climate Change Initiative (CCI). Their land cover raster product documents consistent global land cover coverage at 300 meters spatial resolution on an annual basis from 1992 to 2020, describing the land surface in the 22 classes defined by the United Nations Land Cover Classification System (LCCS). We extract the share of urban land cover from the original compound land cover raster data. Similar to nightlights, for the national level analysis, we adjust for the curvature of Earth for this data as well.[8]

3.2 Nightlights

The baseline nightlights data are derived from annual composites of nightlights intensity from the Defense Meteorological Satellite Program (DMSP) satellites. The stable lights product, available over 1992-2013, provides 6-bit digital numbers (DN) ranging from 0 to 63 for each 30 arc-second output pixel. During processing, ephemeral lights, such as from fires and gas flaring, are removed. Processing also excludes (at the pixel level) images for nights affected by clouds, moonlight, sunlight, and other glare. Lights are aggregated at the geographic level of analysis, after applying a correction for the earth's curvature at the country level.[9]

We extend the baseline DMSP data, which officially ends in 2013 with the decommissioning of the DMSP mission, with a DMSP-like nighttime lights product derived from the Visible Infrared Imaging Radiometer Suite (VIIRS) Lights, and made available by the Earth Observation Group through 2019. In this series, the light product from the VIIRS instrument suite onboard the current NASA /

[8]The ESA-CCI land cover product is an ideal candidate for a signal because it is annually available for an extended period. Hua et al. (2018) find that among commonly used global-scale land cover products, it offers the best spatial consistency over time.

[9]Because of the earth's curvature, grid cell size varies in proportion to the cosine of latitude. We follow HSW's procedure by calculating a weighted average (based on country's land area) of lights across pixels within a country.

NOAA SNPP satellite — which features higher resolution and better overall quality compared to the original DMSP iteration — were converted to DMSP DNs using the methodology by Nechaev et al. (2021).

3.3 GDP

For our national level analysis, official country GDP data at national level are derived from the 2023 World Development Indicators (WDI) dataset of the World Bank. We use constant 2015 US dollar denominated GDP figures.

4 Application

In this section, we illustrate the application of our method with urban land cover as a third signal. We first show that a model with the official GDP, nightlights, and urban land cover as signals satisfies the identification requirements of Section 2.3. We then discuss the results of our estimation for all and African countries.

4.1 Urban Land Cover as a Third Signal

4.1.1 Urban Land Cover and Economic Activities

We first show that the urban land cover signal meaningfully captures economic activities. Figure 1 plots urban land cover growth, x_3, against official GDP growth, x_1, and compares it to the same plot for nightlights luminosity growth, x_2. The growth rates are constructed as log-differences, taking the means of the first and last two years of the period as initial and final observations respectively over the period 1995-2019 for the global sample. We fit a non-parametric regression estimated with an Epanechnikov kernel and bandwidth set at $.8$ to check for non-linearity. Both signals are positively correlated with the official GDP growth, but urban land cover exhibits a weaker correlations than nightlights. We observe very

limited evidence of nonlinear effects, with some nonlinearity mostly driven by the smaller number of observations at the extremes of the signal ranges, especially for urban land cover.

We then estimate the GDP growth predictive regression of model (8). Table 1 reports the estimates of the model for all and African countries, along with predictive regressions based on only either of the two signals alone reflecting the exercise in Figure 1. The predictive regression captures the long-term correlation between GDP growth and the signals. Our methodology is mostly agnostic regarding the predictive stage of the HSW model. It simply requires an additional informative signal with the aforementioned statistical characteristics regardless of the relative magnitude of its coefficient in model (8). The model fit, captured by the adjusted R^2, does not necessarily increase with the additional signal.

4.1.2 The Orthogonality of the ME Errors

Section 2.3 shows that identification first requires the orthogonality of the ME errors for all three signals. Because the three-signal model is just identified, this assumption is untestable. However, we argue that this is a reasonable assumption for our combination of signals.

First, the ME errors may be correlated if, e.g., all signals were collected by the same instrument. However, as discussed in Section 3, official GDP, nightlights and urban land cover were produced by different agencies. The latter two were collected by different satellite programs.

Second, Henderson et al. (2012, p.1006) point out that the errors in the nightlights equation can include cross-country variations in the relationship between official GDP and luminosity growth that arise from the variations in the sectoral compositions of national GDPs. To use their example, while steel and software productions both increase GDP, the former contributes more to luminosity growth than the latter. However, it is reasonable to think these errors are uncorrelated with

errors in the official GDP measurements. We can make a similar argument for the ME errors of urban land cover and official GDP.

Finally, the ME errors of urban land cover and nightlights also differ because the former can only grow horizontally on the map, while the latter can also grow vertically (capturing its intensity). Consider two similar urban expansions that occur either: (i) artificially without economic and population expansions; or (ii) normally with an economic expansion. The nightlights growth from (i) would be feebler than those from (ii). While the ME errors in the urban signal equation is smaller in (ii), the adjustment on the intensive margin of lights might still over-/under-estimate the true GDP growth, decoupling the ME errors of the two signals. Moreover, at the intensive margin, the ME errors of nightlights would be also affected by other factors such as overglow or saturation of the signal, which do not affect urban land cover.

4.1.3 Examining the Signal Covariance Structure

Finally, we examine whether the signals are sufficiently informative for the analysis. Columns 1–3 of Table 2 present the signals' covariance structure for all and African countries. We find that the nightlights-urban land cover correlation is smaller than both the nightlights–official GDP and the urban land cover–official GDP correlations. Nevertheless, it is positive and quite sizable, as expected from conditions (19) and (20).[10]

4.2 Results

We next present the optimal weight for the official GDP growth, λ^*, in equation (11) for our two samples. Table 2 summarizes the overall results. Appendix Table

[10]Overall, the requirements are based on a comparison of variances and covariances of the signals. However, as shown in Appendix B.1, conditions (19) and (20) can also be expressed in correlation terms. We prefer to rely on correlations in the discussion here because they provide the intuition and are easier to interpret.

C.1 reports the full set of estimated parameters and covariance matrices.

4.2.1 All Countries

Our first sample parallels the HSW's exercise.[11] We estimate a $\lambda^* = .56$ for the entire group of countries. The corresponding signal-to-noise ratio of the GDP signal ϕ in (6) is $.78$. This sample includes a large variety of countries, and we can think of this λ as a broadly defined reference value at national level that would work in general for countries with "average" GDP data quality. Following HSW, we split the sample of countries into two based on the World Bank classification of the capacity of their national statistical agencies.[12] For the countries with low-quality statistical capacity we obtain $\lambda^* = .20$ and $\phi = .40$, whereas the high-quality ones have $\lambda^* = .82$ and $\phi = .93$.[13]

Our estimates validate the calibration exercise of HSW by showing that the optimal GDP weight λ^* is an increasing function of the GDP data quality and that nightlights luminosity and urban land cover are useful signals to recover the true economic activity when the GDP data is unreliable. However, the major difference — and the contribution — of our approach is that the augmented models for the two groups are independently identified. Our approach does not require an initial guess to calibrate the signal-to-noise ratio of the official GDP growth signal for either group. Instead, it allows the data to produce a high λ for the countries with high-quality statistical capacity, implying that their GDP data already provide an excellent proxy for economic activity.

[11] Appendix Table C.4 lists the included countries and their GDP data quality. Compared to HSW, we extend the sample by twenty countries, but lose six due to missing GDP observations (see Appendix A.3 for the details). The time period is also extended by thirteen years.

[12] See Appendix A for the data source for the statistical capacity score.

[13] As in HSW, this exercise assumes that the two groups have different signal-to-noise ratios for the official GDP growth signal, while the relation between the other two signals and the official GDP is taken as common across groups.

4.2.2 African Countries

This sample includes developing countries in the lower-to-mid range of GDP data reliability.[14] As in the full sample, the correlation between nightlights and urban land cover is positive, but smaller than the nightlights–official GDP and urban land cover–official GDP correlations. This is consistent with the conditions for the existence of a solution. The optimal estimated weight is $\lambda^* = .38$, with a corresponding signal-to-noise ratio of the GDP growth signal of $\phi = .59$. This result corroborates the notion that the key determinant of λ is the quality of the a country's national accounting system instead of the degree of its development.

5 Empirical Implications

A fully identified model offers the following advantages for empirical work. First, the optimal identification of λ^* yields an accuracy gain that cannot be achieved by adding signals to the GDP growth prediction estimation. Second, under a reasonable assumption, it allows researchers to estimate true GDP growth for the whole sample, even when the third signal is only available for its subset. Third, it provides a means to validate and assess the magnitude and direction of potential measurement errors of empirical applications of signal-based estimation of economic activity. Finally, it offers a criterion to choose between available signals.

5.1 Model Accuracy

We first compare the predicted GDP growth from equation (8), $\hat{x_{1j}}$, with the estimated true GDP growth, $\hat{y_j}$ in (4). Both estimates use the three-signal model specification. We calculate the root mean squared error (RMSE) of using $\hat{x_{1j}}$ instead of $\hat{y_j}$ to predict growth in the full sample of countries. We find an RMSE of 17% —

[14] Appendix Table C.5 lists the included African countries.

a large error that is about one fifth of the average estimated $\hat{y}_j = 83\%$ over the 24 years of our sample.

Next, we show that the accuracy gain from adding an extra signal in the predictive stage is marginal compared to that from properly identifying λ^*. To this end, we compare the optimal $\hat{y}_i$ from the fully-identified three-signal model to that of the nested two-signal model identified by using the subset $(\sigma_y^2, \sigma_1^2, \sigma_2^2, \beta_{x_2})$ of the parameters from the three-signal model. Figure 2 compares the two series for all countries. The two estimates are very similar. They positively comove and a formal t-test does not reject the hypothesis that the difference between the two is zero (with p-value = 1). This confirms that adding the urban signal in the predictive stage leads to a negligible gain in accuracy of $\hat{y}_i$.[15]

Finally, we show that achieving full identification is paramount for the accuracy of the true GDP growth estimates by estimating $\hat{y}_j$ for the countries with low-quality statistical capacity using the overall $\lambda^* = .56$ instead of the group-specific parameter $.20$. We find that this alternative growth prediction would incur an RMSE of 11%, which corresponds to about one seventh of the average growth of 79% estimated for this sample of countries with the correct weights.

5.2 Extrapolation Using an Estimated λ^*

There will be cases where the third signal is not available for a subset of countries. We can combine this approach with HSW's split-sample strategy to estimate economic activity for these countries. We show in Appendix B.3 that under the assumption that two groups of countries differ only in terms of their signal-to-noise ratios of the official GDP growth signal, the availability of a third signal for one group is sufficient to also identify σ_y and λ^*_{HSW} (the optimal weight for the two-signal model) for the group that is missing the third signal. This λ^*_{HSW} would

[15] Appendix Figure C.1 shows a similar comovement of $\hat{y}_i$ constructed using the λ^* from the fully identified three-signal model, and either the three-signal predicted GDP (equation 8) or the two-signal one (equation 3).

allow us to construct an estimate of economic activity growth only relying on the nightlights signal which, as discussed above, would be fairly close to that obtained from the augmented model.

5.3 Model Validation and Measurement Errors

A common empirical application of the HSW framework is to use the predictive stage to estimate GDP growth from nightlights changes. The baseline $\hat{\psi_{x_2}} = .3$ found by HSW is sometimes used; alternatively, when official income data are available for a subset of countries or regions, the predictive model is fitted and the estimated $\hat{\psi_{x_2}}$ applied to the remaining part of the sample (e.g., Civelli et al., 2018).

We can use true GDP growth estimates from the augmented model to assess this practice by comparing the predicted GDP growth, $\hat{x_1}$, to the true GDP growth, $\hat{y}$. First, we randomly select two-thirds of a sample as a training sample to estimate $\hat{\psi_{x_2}}$. We then use it to predict the GDP growth for the remaining third "out-of-sample" observations. We do this for one hundred times, take the average predicted GDP growth for each unit, and compare it with the estimated true GDP growth. We work with the African sample and Figure 3 presents this comparison with the countries grouped by quality of the official GDP data.

The results show that the predicted GDP growth generally underestimates the true GDP growth, with the exception of a handful of lower- and medium-data-quality countries. The estimation error is also substantial, with an RMSE about half the size of the average true GDP growth. In some cases, relying on the predicted GDP growth can lead to quite large errors of up to 3-4% in annualized terms, not only for the lower-data-quality countries (Zimbabwe, Central African Republic) but also the higher-data-quality ones (Ethiopia, Uganda, Nigeria, Malawi). For one country, Equatorial Guinea, the error almost gets as large as 7%.

5.4 Signal Selection

With increased accessibility to geospatial data, researchers might find multiple signals that satisfy the identification conditions (Section 2.3) and can be a viable third signal. We propose a simple theoretical criterion to compare their performance based on the variance of the forecast error of the true GDP growth in (9). This is the loss function that is minimized to find the optimal solution for λ^* and it is a function of the estimated parameters of the fully-identified model. The best third signal, conditional on two other signals, is the one that delivers the lowest forecast error variance.

As an instructive example, we apply this criterion to compare urban land cover to NO_2 emission over the period 2005-2019 for all countries. NO_2 has been demonstrated to be another good predictor of true GDP growth. We use NO_2 emission data based on readings from the Ozone Monitoring Instrument (OMI) of the NASA EOS-Aura satellite.[16] We find that the urban land cover signal is preferred to NO_2 emissions in this sample, with 1.28% v. 1.43% variances, respectively.[17]

However, there can be other empirical considerations for signal selection. For instance, the validation exercise in Section 5.3 can produce a useful criterion. If this is the application of interest, the researcher should consider the signal that delivers the smallest RMSE in the out-of-sample prediction of GDP growth. Similarly, since identification requires the orthogonality of the ME errors, the researcher should consider the extent to which alternative signals satisfy this assumption.

[16] Appendix A details the data source for NO_2 emission.

[17] The time period of this example is dictated by the availability of the NO_2 data. We report the full set of results for the two models estimated for this exercise in Appendix Tables C.2-C.3 and Figure C.2. Overall the two signals perform very similarly, but urban land cover is slightly more informative about nightlights and official GDP as suggested by the comparison criterion.

6 Conclusion

From policy evaluation to international comparisons, the availability of reliable measures of income is of paramount importance for empirical work. We want to be able to accurately infer true income growth. The augmented three-signal model we propose enhances the HSW methodology by solving the identification issue of their original approach. This improvement has relevant implications for the estimation of true GDP growth.

The real gain in accuracy comes from the identification stage of the model, rather than a more refined GDP growth predictive equation. When an official measure of GDP is available, especially when we have little confidence about the quality of the data, using the fully identified model to estimate true GDP growth is crucial. The optimal λ^* varies across samples and geographic level of analysis, and the augmented model can help to correctly choose the optimal λ^* to use to form the estimates.

However, the augmented model is also useful when an official measure of income is only partially available. The augmented model can be leveraged to enhance existing estimation procedures and to validate the estimates produced by other approaches, assessing the sign and magnitude of their potential measurement errors. The flexibility of the augmented model would accommodate other types of third signals instead of urban land cover, such as air pollution or cellular phone data. In principle, the model could also be applied to any other three-signal combinations that do not necessarily include official income statistics or nightlights.

References

Alesina, Alberto, Stelios Michalopoulos, and Elias Papaioannou, "Ethnic Inequality," *Journal of Political Economy*, 2016, *124* (2), 428–488.

Baragwanath, Kathryn, Ran Goldblatt, Gordon Hanson, and Amit K. Khandelwal, "Detecting urban markets with satellite imagery: An application to India," *Journal of Urban Economics*, 2021, *125*, 103173. Delineation of Urban Areas.

Beyer, Robert Carl Michael, Esha Chhabra, Virgilio Galdo, and Martin G. Rama, "Measuring districts'monthly economic activity from outer space," Policy Research Working Paper Series 8523, The World Bank Jul 2018.

Bickenbach, Frank, Eckhardt Bode, Peter Nunnenkamp, and Mareike Söder, "Night lights and regional GDP," *Review of World Economics*, May 2016, *152* (2), 425–447.

Bluhm, Richard and Gordon C. McCord, "What Can We Learn from Nighttime Lights for Small Geographies? Measurement Errors and Heterogeneous Elasticities," *Remote Sensing*, 2022, *14* (5), 1–25.

Boersma, K. F., H. J. Eskes, R. J. Dirksen, R. J. van der A, J. P. Veefkind, P. Stammes, V. Huijnen, Q. L. Kleipool, M. Sneep, J. Claas, J. Leitão, A. Richter, Y. Zhou, and D. Brunner, "An improved tropospheric NO_2 column retrieval algorithm for the Ozone Monitoring Instrument," *Atmospheric Measurement Techniques*, 2011, *4* (9), 1905–1928.

Chen, X. and W. D. Nordhaus, "Using luminosity data as a proxy for economic statistics," *Proceedings of the National Academy of Sciences*, May 2011, *108* (21), 8589–8594.

Civelli, Andrea, Andrew Horowitz, and Arilton Teixeira, "Foreign aid and growth: A Sp P-VAR analysis using satellite sub-national data for Uganda," *Journal of Development Economics*, 2018, *134*, 50 – 67.

Dai, Zhaoxin, Yunfeng Hu, and Guanhua Zhao, "The suitability of different nighttime light data for GDP estimation at different spatial scales and regional levels," 2017.

Dreher, Axel and Steffen Lohmann, "Aid and Growth at the Regional Level," IMF Working Papers 15/196, International Monetary Fund September 2015.

Engstrom, Ryan, Jonathan Hersh, and David Newhouse, "Poverty from Space: Using High Resolution Satellite Imagery for Estimating Economic Well-being," *The World Bank Economic Review*, 07 2021, *36* (2), 382–412.

Ezran, Irene, Stephen D. Morris, Martín Rama, and Daniel Riera-Crichton, "Measuring Global Economic Activity Using Air Pollution," World Bank Policy Research Working Paper 10445 2023.

Ghosh, Tilottama, Rebecca L. Powell, Christopher D. Elvidge, Kimberly E. Baugh, Paul C. Sutton, and Sharolyn Anderson, "Shedding Light on the Global Distribution of Economic Activity," *The Open Geography Journal*, 2010, *3* (3), 148–61.

Gibson, John and Geua Boe-Gibson, "Nighttime lights and county-level economic activity in the United States: 2001 to 2019," *Remote Sensing*, 2021, *13* (14).

Goldblatt, Ran, Kilian Heilmann, and Yonatan Vaizman, "Can Medium-Resolution Satellite Imagery Measure Economic Activity at Small Geographies? Evidence from Landsat in Vietnam," *The World Bank Economic Review*, 10 2019, *34* (3), 635–653.

Henderson, J. Vernon, Adam Storeygard, and David N Weil, "Measuring Economic Growth from Outer Space," *American Economic Review*, April 2012, *102* (2), 994–1028.

Hodler, Roland and Paul A. Raschky, "Regional Favoritism," *The Quarterly Journal of Economics*, 03 2014, *129* (2), 995–1033.

Hua, Ting, Wenwu Zhao, Yanxu Liu, Shuai Wang, and Siqi Yang, "Spatial Consistency Assessments for Global Land-Cover Datasets: A Comparison among GLC2000, CCI LC, MCD12, GLOBCOVER and GLCNMO," *Remote Sensing*, 2018, *10* (11).

Keola, Souknilanh, Magnus Andersson, and Ola Hall, "Monitoring Economic Development from Space: Using Nighttime Light and Land Cover Data to Measure Economic Growth," *World Development*, 2015, *66*, 322 – 334.

Lehnert, Patrick, Michael Niederberger, Uschi Backes-Gellner, and Eric Bettinger, "Proxying Economic Activity with Daytime Satellite Imagery: Filling Data Gaps Across Time and Space," Economics of Education Working Paper Series 0165, University of Zurich, Department of Business Administration (IBW) Mar 2020.

Maldonado, Leonardo, "Lighting-up the economic activity of oil-producing regions: A remote sensing application," *Remote Sensing Applications: Society and Environment*, 2022, *26* (March), 100722.

Michalopoulos, Stelios and Elias Papaioannou, "National Institutions and Subnational Development in Africa," *The Quarterly Journal of Economics*, 12 2013, *129* (1), 151–213.

_ **and** _ , "Pre-Colonial Ethnic Institutions and Contemporary African Development," *Econometrica*, 2013, *81* (1), 113–152.

Morris, Stephen D. and Junjie Zhang, "Validating China's Output Data Using Satellite Observations," *Macroeconomics Dynamics*, 2019, *23*, 3327–3354.

Nechaev, Dmitry, Mikhail Zhizhin, Alexey Poyda, Tilottama Ghosh, Feng-Chi Hsu, and Christopher Elvidge, "Cross-Sensor Nighttime Lights Image Calibration for DMSP/OLS and SNPP/VIIRS with Residual U-Net," *Remote Sensing*, 2021, *13* (24).

Pinkovskiy, Maxim and Xavier Sala i Martin, "Lights, Camera ... Income! Illuminating the National Accounts-Household Surveys Debate," *The Quarterly Journal of Economics*, 2016, *131* (2), 579–631.

_ **and** _ , "Newer Need Not be Better: Evaluating the Penn World Tables and the World Development Indicators Using Nighttime Lights," Working Paper 22216, National Bureau of Economic Research May 2016.

Storeygard, Adam, "Farther on down the Road: Transport Costs, Trade and Urban Growth in Sub-Saharan Africa," *The Review of Economic Studies*, 04 2016, *83* (3), 1263–1295.

Wang, Xuantong, Mickey Rafa, Jonathan D Moyer, Jing Li, Jennifer Scheer, and Paul Sutton, "Estimation and Mapping of Sub-National GDP in Uganda Using NPP-VIIRS Imagery," *Remote Sensing*, January 2019, p. 163.

Wu, Jiansheng, Zheng Wang, Weifeng Li, and Jian Peng, "Exploring factors affecting the relationship between light consumption and GDP based on DMSP/OLS nighttime satellite imagery," *Remote Sensing of Environment*, 2013, *134*, 111 – 119.

Zhang, Xiaoxuan and John Gibson, "Using Multi-Source Nighttime Lights Data to Proxy for County-Level Economic Activity in China from 2012 to 2019," *Remote Sensing*, 2022, *14* (5).

Tables and Figures

Table 1: Official GDP Growth (x_1) Predictive Regressions

	World			**Africa**		
	(1)	(2)	(3)	(4)	(5)	(6)
$nighlights$ (x_2)	0.413	0.461		0.241	0.283	
	(0.054)	(0.046)		(0.098)	(0.095)	
$urban$ (x_3)	0.185		0.393	0.258		0.435
	(0.074)		(0.100)	(0.139)		(0.161)
N	184	184	184	45	45	45
adj. R^2	0.486	0.455	0.166	0.293	0.263	0.128
Period	1995-2019	1995-2019	1995-2019	2001-2019	2001-2019	2001-2019

Note: Estimation of the predictive regression model (8). Growth rates are calculated as log-differences over the sample, taking the mean of the observations of the first and last two years of the sample as initial and final values. Columns (2) and (5) report the estimates of the regression in the corresponding HSW two-signal version of the model in equation (3). Columns (3) and (6) correspond to the two-signal model with the urban land cover signal instead of nightlights. Robust standard errors in parentheses.

Table 2: Signal Correlations and Model Parameters

	$\rho_{x_1x_2}$	$\rho_{x_1x_3}$	$\rho_{x_2x_3}$	ϕ	λ^*
	(1)	(2)	(3)	(4)	(5)
All Countries	0.68	0.41	0.36	0.78	0.56
Countries with [...] statistical capacity:					
– high-quality				0.93	0.82
– low-quality				0.40	0.20
African Countries	0.53	0.38	0.35	0.59	0.38

Note: Signal correlation structure and estimates of λ^* (the optimal GDP growth weight in 11) and ϕ (the signal-to-noise ratio of the GDP growth signal defined in 6) in the augmented model for the two samples of analysis. The notation $\rho_{x_ix_j}$ indicates the correlation between signal x_i and x_j. A common correlation structure is maintained across the subsets of countries with high- and low-quality statistical capacity.

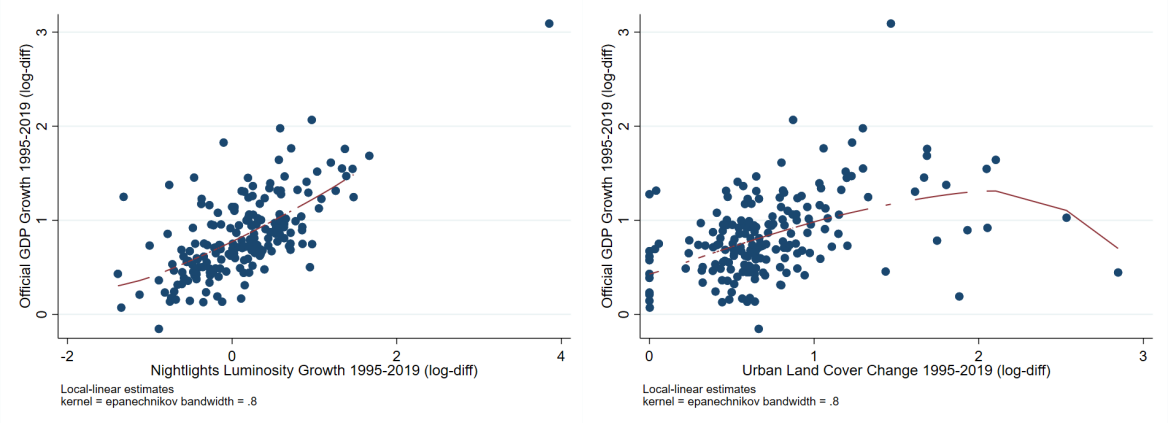

(a) Nightlights (b) Urban land cover

Note: Long-term comparison of the growth rates of official GDP and nightlights luminosity (Panel a) and GDP and urban land cover (Panel b). Growth rates are calculated as log-differences over the sample, taking the mean of the observations of the first and last two years of the sample as initial and final values. Full World countries sample for the period 1995-2019. The red lines correspond to a non-parametric, local-linear fit estimated with an Epanechnikov kernel (bandwidth = .8).

Figure 1: Official GDP Growth v. Signals Growth

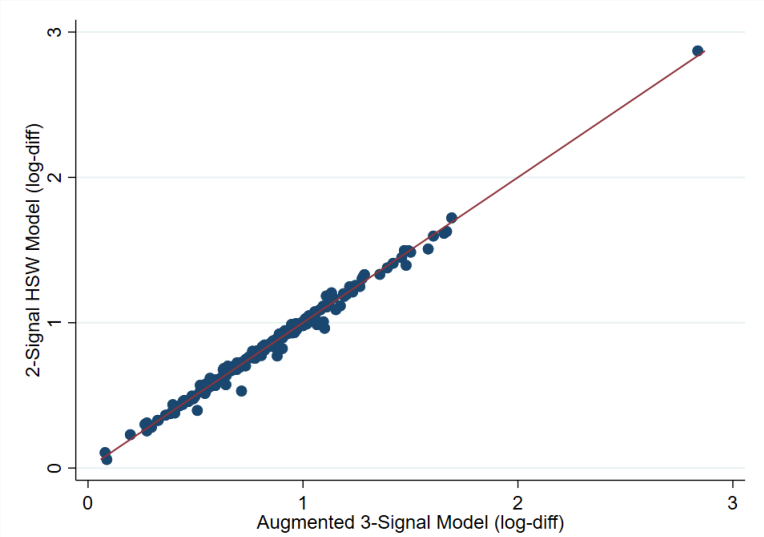

Note: Comparison of the estimated true GDP growth $\hat{y}_i$ from the augmented model (with x_2 and x_3 signals) with that from the HSW two-signal model (with x_2 only). The full set of parameters are identified using the three-signal model, and the subset $(\sigma_y^2, \sigma_1^2, \sigma_2^2, \beta_{x_2})$ of those parameters are used to estimate the two-signal model. The solid line is the 45-degree line. Sample is all countries.

Figure 2: True Growth Estimates: Two- v. Three-Signal Model

Note: Comparison of the out-of-sample prediction of GDP growth based on the nightlights signal only (x_2) with the true GDP growth estimated with the three-signal model. Two thirds of the observations are used as the training sample to estimate the $\hat{\psi_{x_2}}$ that is used to predict GDP growth for the remaining "out-of-sample" observations. Average predicted GDP growth is reported out of one hundred repetitions. The solid line is the 45-degree line. Sample is the African countries.

Figure 3: Out-of-sample Predicted GDP v. Model-Estimated True GDP Growth

Online Appendix

A Dataset

This section provides further details on the additional datasets used in the empirical exercise and how the all country sample is constructed.

A.1 Nitrogen Dioxide

To illustrate our signal selection criterion (Section 5.4), we use satellite readings of tropospheric nitrogen dioxide (NO_2) densities as an alternative third signal. NO_2 is a byproduct of anthropogenic sources primarily including combustion, and thus directly representative of economic activity. The short atmospheric lifespan of NO_2, at less than a day, would imply that densities are closely correlated to anthropogenic emissions. While these densities may be subject to other non-human factors (e.g., soil emissions, wildfires, and lightning), these would have comparatively small effects.[18]

The NO_2 data in this paper are based on readings from the Ozone Monitoring Instrument (OMI), a nadir-viewing visual and ultraviolet spectrometer aboard the NASA EOS-Aura satellite, for the period 2005-2020 and elaborated by Boersma et al. (2011).[19] Similar to the data for nightlights and urban land cover, we also adjust them for the Earth's curvature.

A.2 Statistical Capacity Score

Following HSW, we demarcate the countries used in our analysis based on the robustness of their respective statistical capacities. We use the World Bank's Statistical Capacity Indicators from 2010. It is a composite score that captures the

[18] For a comprehensive assessment of the use of NO_2 for the estimation of economic activities see Ezran et al. (2023).

[19] NO_2 are publicly, freely available from different online sources. We obtain them from the ESA Tropospheric Emission Monitoring Internet Service at http://www.temis.nl/.

capacity of a country's statistical system in the following areas: methodology; data sources; and periodicity and timeliness. Countries are scored against 25 criteria in these areas, using publicly available information and/or country input. The overall score is a simple average of all three area scores on a scale of 0-100. We use a cutoff of 50 to distinguish between countries with high and low statistical capacity.

A.3 All Countries Sample

Compared to the sample in the HSW's long-difference analysis, our sample:

- Includes 20 additional countries: Aruba, Andorra, Bahrain, Bosnia and Herzegovina, Barbados, Cuba, Equatorial Guinea, Hong Kong, Iraq, Kuwait, Macao, Monaco, Maldives, New Caledonia, Puerto Rico, Palestina, French Polynesia, Singapore, Serbia, and Tuvalu.
- Drops 6 countries due to missing GDP data either at the beginning or the end of the time sample: Djibouti, Liberia, Palau (at the beginning of the sample); Eritrea, Venezuela, Yemen (at the end of the sample).

B Theoretical Methods

This section provides further details on some of the theoretical results in Section 2.

B.1 Solving the Augmented Model

In this section, we derive the solution of the augmented model. It also presents the set of technical conditions that must be empirically satisfied by the signals to solve for the parameters of the model.

The Solution: The identifying moment conditions derived in the paper (equations 12-17) are:

$$\sigma_{x_1}^2 = \sigma_y^2 + \sigma_1^2 \tag{B.1}$$

$$\sigma_{x_2}^2 = \beta_{x_2}^2 \sigma_y^2 + \sigma_2^2 \tag{B.2}$$

$$\sigma_{x_3}^2 = \beta_{x_3}^2 \sigma_y^2 + \sigma_3^2 \tag{B.3}$$

$$\sigma_{x_1 x_2} = \beta_{x_2} \sigma_y^2 \tag{B.4}$$

$$\sigma_{x_1 x_3} = \beta_{x_3} \sigma_y^2 \tag{B.5}$$

$$\sigma_{x_2 x_3} = \beta_{x_2} \beta_{x_3} \sigma_y^2. \tag{B.6}$$

From the last three moment conditions (B.4)-(B.6), we can obtain the solution for β_{x_2}, β_{x_3}, and σ_y^2:

$$\sigma_y^2 = \frac{\sigma_{x_1 x_3} \sigma_{x_1 x_2}}{\sigma_{x_2 x_3}} \tag{B.7}$$

$$\beta_{x_2} = \frac{\sigma_{x_2 x_3}}{\sigma_{x_1 x_3}} \tag{B.8}$$

$$\beta_{x_3} = \frac{\sigma_{x_2 x_3}}{\sigma_{x_1 x_2}}. \tag{B.9}$$

Using these solutions into (B.1)-(B.3), we find the solution for the remaining three parameters:

$$\sigma_1^2 = \sigma_{x_1}^2 - \frac{\sigma_{x_1 x_3} \sigma_{x_1 x_2}}{\sigma_{x_2 x_3}} \tag{B.10}$$

$$\sigma_2^2 = \sigma_{x_2}^2 - \sigma_{x_1 x_2}^2 \tag{B.11}$$

$$\sigma_3^2 = \sigma_{x_3}^2 - \sigma_{x_1 x_3}^2. \tag{B.12}$$

Technical Requirements: There are four empirical requirements for a solution to exist. First, a third signal must be positively correlated with the second one. The relation between signals and true economic activity can be normalized, without loss of generality, to be positive, that is $\beta_{x_2}, \beta_{x_3} > 0$. This implies that $\sigma_{x_1 x_2}$ and

$\sigma_{x_1x_3}$ must be positive in (B.4)-(B.5). Therefore, given the solution for σ_y^2, also

$$\sigma_{x_2x_3} > 0. \tag{B.13}$$

The other three requirements come from (B.10)-(B.12):

$$\sigma_{x_1}^2 > \frac{\sigma_{x_1x_3}\sigma_{x_1x_2}}{\sigma_{x_2x_3}} \tag{B.14}$$

$$\sigma_{x_2}^2 > \sigma_{x_1x_2}^2 \tag{B.15}$$

$$\sigma_{x_3}^2 > \sigma_{x_1x_3}^2. \tag{B.16}$$

These three conditions simply require that the three signals exhibit sufficiently high variance relative to the observed signal covariance structure. While we find that conditions (B.15) and (B.16) are generally easily satisfied by the data, condition (B.14) more closely depends on the covariance between second and third signals. The higher $\sigma_{x_2x_3}$, the easier the requirement is satisfied. Hence, a positive and sufficiently strong covariance between second and third signals is the key condition to empirically select the third signal.

We also note that condition (B.14) can be easily rewritten in terms of correlations between signals:

$$\frac{\rho_{x_1x_3}\rho_{x_1x_2}}{\rho_{x_2x_3}} < 1, \tag{B.17}$$

where the notation $\rho_{x_ix_j}$ indicates the correlation between signal x_i and x_j. Similarly, condition (B.13) can be re-expressed in correlation terms as $\rho_{x_2x_3} > 0$. We refer to (B.17) in the discussion of the empirical implementation of the model in Section 4.1.3.

B.2 Higher-order Augmentation

Although the scope of this paper revolves around the fully-identified three-signal model, we can extend the framework to any $N \geqslant 2$ signals. Let the index $n = 1, ..., N$ indicate the signals, the structure of the model comprises N measurement

equations:

$$x_{1j} = \beta_{x_1} y_j + \varepsilon_{1j}$$
$$x_{nj} = \beta_{x_n} y_j + \varepsilon_{nj} \quad \forall n = 2, ..., N,$$

and the predictive equation:

$$x_{1j} = \sum_{n=2}^{N} \psi_{x_n} x_{nj} + e_j.$$

The vector of unknown parameters includes $2N$ coefficients $(\sigma_y^2, \{\sigma_n^2\}_{n=1}^N, \{\beta_{x_n}\}_{n=2}^N)$, with a total number of $\frac{N(N+1)}{N}$ moment conditions – given by the N variances of the signals and by the $\frac{N!}{2(N-2)!}$ covariances between all possible pairs of signals. The N-signal model is hence over-identified by $\frac{N(N-3)}{2}$ moment conditions.

The optimal λ^* follows an expression equivalent to (10)

$$\lambda^* = \frac{\hat{\psi}_{x_2}^2 \sigma_2^2 + \cdots + \hat{\psi}_{x_N}^2 \sigma_N^2 + \left(\hat{\psi}_{x_2}\beta_{x_2} + \cdots + \hat{\psi}_{x_N}\beta_{x_N} - 1\right)^2 \sigma_y^2}{\sigma_1^2 + \hat{\psi}_{x_2}^2 \sigma_2^2 + \cdots + \hat{\psi}_{x_N}^2 \sigma_N^2 + (\hat{\psi}_{x_2}\beta_{x_2} + \cdots + \hat{\psi}_{x_N}\beta_{x_N} - 1)^2 \sigma_y^2},$$

but the vector of unknown coefficients does not have a simple closed-form solution anymore and must be estimated, for instance, by GMM.

The over-identification result relies on the orthogonality assumption of the errors terms ε_n. If this assumption is relaxed, $\frac{N(N-1)}{2}$ structural parameters would be added to the model and the identification would be short by N moment conditions. This assumption may be more convincing for some signal pairs, but not others. In such a case, a model with multiple signals which is over-identified under this underlying assumption could provide a way to pin down some of these pairwise correlations.

Moreover, the over-identification of an N-signal model could be exploited to device a test for the orthogonality assumption in the nested three-signal model. The basic idea of this test would be to compare the estimated $\hat{y}_j$ from the two versions of the model and test whether the difference between the two is statistically

significant. In a manner similart to the Hansen-Sargan test, however, the rejection of the test would not allow us to know which signal pairs fail the assumption.

Finally, as for the three-signal model, the N signals must empirically satisfy some requirements for the signals to be admissible. In particular, the signal covariance structure in the data must allow for a solution of the parameters of the model in a space in which the signal to noise ratios are smaller than 1, i.e., in which the estimated measurement equations error variances are necessarily positive. In our empirical investigation of the thee-signal model, we find this condition is not always easily satisfied by any signal. Increasing the number of auxiliary signals, we expect these requirements to be even more challenging to satisfy.

B.3 Solution for the Split-Sample Model

This section provides details on the split-sample approach discussed in Section 2 (footnote 6) and Section 5.2, and used in Section 4.1.3 for the heterogeneity analysis by data quality.

Let us suppose that a sample of countries can be split into two group, A and B, based on some characteristics which provides some useful information for identification. In their split-sample exercise, HSW assume that the two groups share the same model equations, except for equation (1) in which the variance of the g signal is allowed to be group specific. The identifying condition (B.1) can be restated as

$$\sigma^2_{x_1,A} = \sigma^2_y + \sigma^2_{1,A} \tag{B.18}$$

$$\sigma^2_{x_1,B} = \sigma^2_y + \sigma^2_{1,B}. \tag{B.19}$$

This assumption also implies that equation (6), the signal to noise ratio of the x_1

signal (i.e., GDP growth in all these applications), must differ by group:

$$\phi_A = \frac{\sigma_y^2}{\sigma_y^2 + \sigma_{1,A}^2} \tag{B.20}$$

$$\phi_B = \frac{\sigma_y^2}{\sigma_y^2 + \sigma_{1,B}^2}. \tag{B.21}$$

By calibrating ϕ_A, an additional condition is provided to solve the HSW's model for group A. In particular σ_y^2 and $\sigma_{1,A}^2$ are obtained. Given σ_y^2, (B.19) pins down $\sigma_{1,B}^2$ and, as a consequence, ϕ_B as well. This is sufficient to also find a solution of the two-signal HSW model for group B. The same approach would apply to the augmented three-signal model, but it is not necessary to find a solution in this case, as the augmented model would already be fully identified for each group separately.

Exploiting this approach, however, the augmented model allows for a further result as we discuss in Section 5.2. Suppose a third signal x_3 is available for group A, but not group B. The augmented model allows us to solve for all the model parameters for group A, especially σ_y^2. Under the assumption of the split-sample approach that σ_y^2 is common across groups, the two-signal model with only signals x_1 and x_2 for group B can be completely identified since only three parameters are left now $(\sigma_1^2, \sigma_2^2, \beta_{x_2})$ with three moment conditions. Moreover, in this case, the remaining parameters could be taken as common across the entire sample (estimating the two-signal model with data from groups A and B) or could even be assumed to be group-specific for group A if preferred.

C Additional Tables and Figures

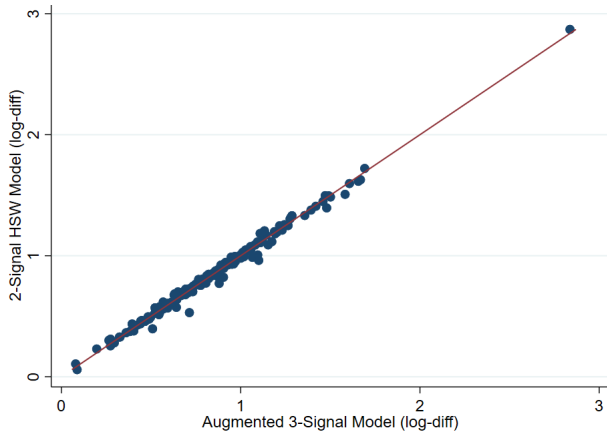

Note: Comparison of the estimated true GDP growth $\hat{y}_i$ obtained from (4) for the augmented three-signal model – with x_2 and x_3 signals used to predict $\hat{x}_1$ – to the $\hat{y}_i$ in which only x_2 is used to predict $\hat{x}_1$ in (4). The solid line is the 45-degree line. Sample is all countries.

Figure C.1: True GDP Growth Estimates

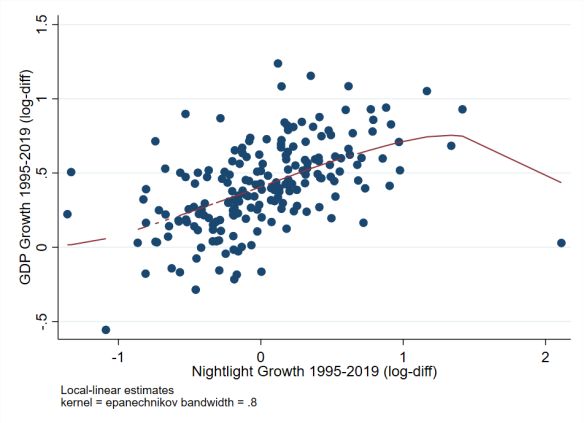

(a) Nightlights

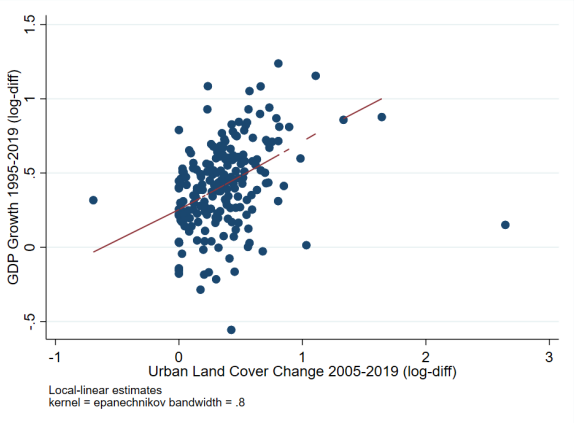

(b) Urban land cover

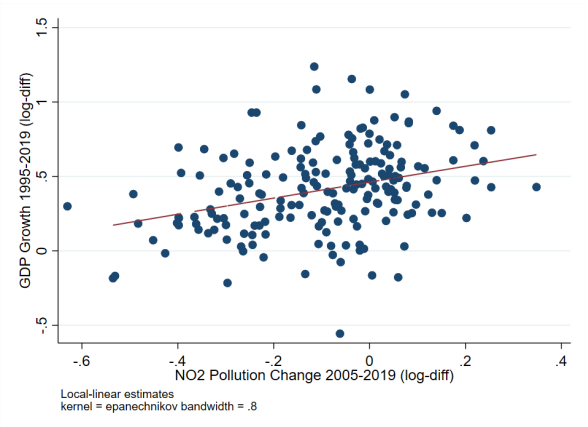

(c) NO_2

Note: Long-term comparison of the growth rates of official GDP and: (a) nightlights luminosity; (b) urban land cover; and (c) NO_2 emission for all countries between 2005 and 2019. Growth rates are calculated as log-differences over the sample, taking the mean of the observations of the first and last two years of the sample as initial and final values. The red lines correspond to a non-parametric, local-linear fit estimated with an Epanechnikov kernel (bandwidth $= .8$).

Figure C.2: Official GDP Growth v. Signals Growth

Table C.1: Model Parameters and the Signal Covariance Structure

Panel A: Parameter Estimations						
Model	β_{x_2}	β_{x_3}	σ_1	σ_2	σ_3	σ_y
All Countries	1.28	0.56	0.04	0.17	0.17	0.15
Countries with [...] statistical capacity:						
– high-quality	1.28	0.56	0.01	0.17	0.17	0.15
– low-quality	1.28	0.56	0.22	0.17	0.17	0.15
African Countries	1.69	0.58	0.04	0.19	0.06	0.06
Panel B: Signal Covariance Structure						
Model	$\sigma^2_{x_1}$	$\sigma^2_{x_2}$	$\sigma^2_{x_3}$	$\sigma_{x_1x_2}$	$\sigma_{x_1x_3}$	$\sigma_{x_2x_3}$
All Countries	0.19	0.41	0.21	0.19	0.08	0.11
Countries with [...] statistical capacity:						
– high-quality	0.16					
– low-quality	0.37					
African Countries	0.11	0.37	0.08	0.10	0.04	0.06

Note: Panel A reports the estimates of the six parameters of the augmented model. Panel B reports the covariance structures of the signals for the two cases analyzed: all and African countries. A common covariance structure is maintained across these two sub-sets, with the exception of $\sigma^2_{x_1}$.

Table C.2: Official GDP Growth (x_1) Predictive Regressions, All Countries, 2005-2019

	NO_2			$urban$		
	(1)	(2)	(3)	(4)	(5)	(6)
$nighlights$ (x_2)	0.254	0.284		0.218	0.284	
	(0.058)	(0.058)		(0.063)	(0.058)	
NO_2 (x_3)	0.367		0.531			
	(0.105)		(0.099)			
$urban$ (x_3)				0.311		0.467
				(0.080)		(0.070)
N	189	189	189	189	189	189
adj. R^2	0.280	0.236	0.100	0.304	0.236	0.187
$Period$	2005-2019	2005-2019	2005-2019	2005-2019	2005-2019	2005-2019

Note: Estimation of the predictive regression model (8) for the 2005-2019 period for all countries. $urban$ and NO_2 respectively indicate the growth rates of urban land cover and nitrogen dioxide pollution, two alternative x_3 signals. Growth rates are calculated as log-differences over the sample, taking the mean of the observations of the first and last two years of the sample as initial and final values. Columns (2) and (5) report the estimates of the regression in the corresponding HSW two-signal version of the model in equation (3). Columns (3) and (6) correspond to the two-signal model with the urban land cover signal/NO_2 instead of nightlights. Robust standard errors in parentheses.

Table C.3: Comparing Two Signals – 2005-2019

Panel A: Signal Correlation and Model Parameters						
Model	$\rho_{x_1x_2}$	$\rho_{x_1x_3}$	$\rho_{x_2x_3}$	ϕ	λ^*	$Loss$
NO_2	0.49	0.32	0.23	0.70	0.57	1.43%
$urban$	0.49	0.44	0.39	0.55	0.35	1.28%
Panel B: Parameter Estimations						
Model	β_{x_2}	β_{x_3}	σ_1	σ_2	σ_3	σ_y
NO_2	1.21	0.28	0.02	0.16	0.03	0.06
$urban$	1.54	0.74	0.04	0.14	0.05	0.05
Panel C: Signal Covariance Structure						
Model	$\sigma^2_{x_1}$	$\sigma^2_{x_2}$	$\sigma^2_{x_3}$	$\sigma_{x_1x_2}$	$\sigma_{x_1x_3}$	$\sigma_{x_2x_3}$
NO_2	0.08	0.24	0.03	0.07	0.02	0.02
$urban$	0.08	0.24	0.07	0.07	0.03	0.05

Note: Parameters and covariance structures of the two three-signal models compared in Section 5.4. The two models are estimated for the sample of all countries, over the period 2005-2019. The two models differ for the third signal used: respectively, NO_2 and urban land cover. Panel A reports the signal correlation structure and estimates of λ^*, ϕ, and the variance of the GDP forecast error ($Loss$). Panel B shows the estimates of the six parameters of the augmented model. Panel C compares the covariance structures of the signals for the two model.

Table C.4: Statistical Capacity of All Countries

Country	Code	Statistical Capacity Score	Low-quality	High-quality
Aruba	ABW	0	1	
Angola	AGO	46	1	
Albania	ALB	70		1
Andorra	AND	100		1
United Arab Emirates	ARE	100		1
Argentina	ARG	87		1
Armenia	ARM	92		1
Antigua and Barbuda	ATG	42	1	
Australia	AUS	100		1
Austria	AUT	100		1
Azerbaijan	AZE	79		1
Burundi	BDI	54		1
Belgium	BEL	100		1
Benin	BEN	56		1
Burkina Faso	BFA	62		1
Bangladesh	BGD	69		1
Bulgaria	BGR	91		1
Bahrain	BHR	100		1
Bahamas	BHS	100		1
Bosnia and Herzegovina	BIH	62		1
Belarus	BLR	86		1
Belize	BLZ	61		1
Bermuda	BMU	100		1
Bolivia	BOL	67		1
Brazil	BRA	83		1
Barbados	BRB	0	1	
Brunei	BRN	100		1
Bhutan	BTN	76		1
Botswana	BWA	60		1
Central African Republic	CAF	56		1
Canada	CAN	100		1
Switzerland	CHE	100		1
Chile	CHL	94		1
China	CHN	66		1
Côte d'Ivoire	CIV	59		1
Cameroon	CMR	67		1
Democratic Republic of the Congo	COD	36	1	
Republic of Congo	COG	54		1
Colombia	COL	84		1

Statistical Capacity of All Countries (continued)

Country	Code	Statistical Capacity Score	Low-quality	High-quality
Comoros	COM	50	1	
Cape Verde	CPV	73		1
Costa Rica	CRI	77		1
Cuba	CUB	99		1
Cyprus	CYP	100		1
Czech Republic	CZE	99		1
Germany	DEU	100		1
Dominica	DMA	47	1	
Denmark	DNK	100		1
Dominican Republic	DOM	68		1
Algeria	DZA	59		1
Ecuador	ECU	82		1
Egypt	EGY	86		1
Spain	ESP	100		1
Estonia	EST	99		1
Ethiopia	ETH	80		1
Finland	FIN	100		1
Fiji	FJI	53		1
France	FRA	100		1
Micronesia	FSM	28	1	
Gabon	GAB	40	1	
United Kingdom	GBR	100		1
Georgia	GEO	96		1
Ghana	GHA	66		1
Guinea	GIN	58		1
Gambia	GMB	68		1
Guinea-Bissau	GNB	46	1	
Equatorial Guinea	GNQ	32	1	
Greece	GRC	100		1
Grenada	GRD	43	1	
Guatemala	GTM	86		1
Guyana	GUY	53		1
Hong Kong	HKG	100		1
Honduras	HND	76		1
Croatia	HRV	84		1
Haiti	HTI	42	1	
Hungary	HUN	87		1
Indonesia	IDN	87		1
Isle of Man	IMN	100		1
India	IND	81		1

Statistical Capacity of All Countries (continued)

Country	Code	Statistical Capacity Score	Low-quality	High-quality
Ireland	IRL	100		1
Iran	IRN	71		1
Iraq	IRQ	41	1	
Iceland	ISL	100		1
Israel	ISR	100		1
Italy	ITA	100		1
Jamaica	JAM	74		1
Jordan	JOR	77		1
Japan	JPN	100		1
Kazakhstan	KAZ	96		1
Kenya	KEN	62		1
Kyrgyzstan	KGZ	89		1
Cambodia	KHM	73		1
Kiribati	KIR	37	1	
Saint Kitts and Nevis	KNA	61		1
South Korea	KOR	100		1
Kuwait	KWT	100		1
Laos	LAO	70		1
Lebanon	LBN	57		1
Saint Lucia	LCA	60		1
Sri Lanka	LKA	77		1
Lesotho	LSO	66		1
Lithuania	LTU	99		1
Luxembourg	LUX	100		1
Latvia	LVA	99		1
Macao	MAC	0	1	
Morocco	MAR	78		1
Monaco	MCO	100		1
Moldova	MDA	84		1
Madagascar	MDG	68		1
Maldives	MDV	66		1
Mexico	MEX	86		1
Marshall Islands	MHL	41	1	
Macedonia	MKD	79		1
Mali	MLI	63		1
Malta	MLT	100		1
Myanmar	MMR	52		1
Mongolia	MNG	74		1
Mozambique	MOZ	72		1
Mauritania	MRT	62		1

Statistical Capacity of All Countries (continued)

Country	Code	Statistical Capacity Score	Low-quality	High-quality
Mauritius	MUS	70		1
Malawi	MWI	79		1
Malaysia	MYS	80		1
Namibia	NAM	52		1
New Caledonia	NCL	0	1	
Niger	NER	68		1
Nigeria	NGA	69		1
Nicaragua	NIC	76		1
Netherlands	NLD	100		1
Norway	NOR	100		1
Nepal	NPL	64		1
New Zealand	NZL	100		1
Oman	OMN	0	1	
Pakistan	PAK	77		1
Panama	PAN	79		1
Peru	PER	81		1
Philippines	PHL	89		1
Papua New Guinea	PNG	41	1	
Poland	POL	86		1
Puerto Rico	PRI	100		1
Portugal	PRT	100		1
Paraguay	PRY	70		1
Palestina	PSE	42	1	
French Polynesia	PYF	0	1	
Romania	ROU	96		1
Russia	RUS	88		1
Rwanda	RWA	68		1
Saudi Arabia	SAU	100		1
Sudan	SDN	44	1	
Senegal	SEN	73		1
Singapore	SGP	100		1
Solomon Islands	SLB	40	1	
Sierra Leone	SLE	52		1
El Salvador	SLV	91		1
Serbia	SRB	76		1
Suriname	SUR	71		1
Slovakia	SVK	83		1
Slovenia	SVN	99		1
Sweden	SWE	100		1
Swaziland	SWZ	68		1

Statistical Capacity of All Countries (continued)

Country	Code	Statistical Capacity Score	Low-quality	High-quality
Seychelles	SYC	59		1
Chad	TCD	57		1
Togo	TGO	51		1
Thailand	THA	80		1
Tajikistan	TJK	74		1
Turkmenistan	TKM	39	1	
Tonga	TON	59		1
Trinidad and Tobago	TTO	71		1
Tunisia	TUN	79		1
Turkey	TUR	84		1
Tuvalu	TUV	0	1	
Tanzania	TZA	68		1
Uganda	UGA	70		1
Ukraine	UKR	88		1
Uruguay	URY	96		1
United States	USA	100		1
Uzbekistan	UZB	61		1
Saint Vincent and the Grenadines	VCT	54		1
Vietnam	VNM	64		1
Vanuatu	VUT	42	1	
Samoa	WSM	49	1	
Yemen	YEM	49	1	
South Africa	ZAF	82		1
Zambia	ZMB	58		1
Zimbabwe	ZWE	51		1

Note: The statistical capacity score is provided by the World Bank for developing countries. We assign a score of 100 by default to developed countries. A cutoff of 50 is used to classify countries as low/high quality.

Table C.5: Statistical Capacity of Included African Countries

Country	Code	Statistical Capacity Score	Low Quality	Medium Quality	High Quality
Angola	AGO	46	1		
Burundi	BDI	54	1		
Benin	BEN	56	1		
Burkina Faso	BFA	62		1	
Botswana	BWA	60		1	
Central African Republic	CAF	56	1		
Côte d'Ivoire	CIV	59		1	
Cameroon	CMR	67		1	
Democratic Rep. of Congo	COD	36	1		
Republic of Congo	COG	54	1		
Algeria	DZA	59		1	
Egypt	EGY	86			1
Ethiopia	ETH	80			1
Gabon	GAB	40	1		
Ghana	GHA	66		1	
Guinea	GIN	58		1	
Gambia	GMB	68		1	
Guinea-Bissau	GNB	46	1		
Equatorial Guinea	GNQ	32	1		
Kenya	KEN	62		1	
Liberia	LBR	33	1		
Libya	LBY	41	1		
Lesotho	LSO	66		1	
Morocco	MAR	78			1
Madagascar	MDG	68		1	
Mali	MLI	63		1	
Mozambique	MOZ	72			1
Mauritania	MRT	62		1	
Malawi	MWI	79			1
Namibia	NAM	52	1		
Niger	NER	68		1	
Nigeria	NGA	69			1
Rwanda	RWA	68		1	
Sudan	SDN	44	1		
Senegal	SEN	73			1
Sierra Leone	SLE	52	1		
Swaziland	SWZ	68		1	
Chad	TCD	57		1	
Togo	TGO	51	1		
Tunisia	TUN	79			1
Tanzania	TZA	68		1	
Uganda	UGA	70			1
South Africa	ZAF	82			1
Zambia	ZMB	58		1	
Zimbabwe	ZWE	51	1		

Note: The statistical capacity score is provided by the World Bank for developing countries. The quality groups are defined by the terciles of the score distribution.